ACS APPLIED MATERIALS & INTERFACES

www.acsami.org Research Article

Green and Tunable Animal Protein-Free Microcarriers for Cell Expansion

Eleana Somville, Anitha Ajith Kumar, Jérôme Guicheux, Boris Halgand, Sophie Demoustier-Champagne, Anne des Rieux,* Alain M. Jonas, and Karine Glinel*

Cite This: https://dx.doi.org/10.1021/acsami.0c16875 Read Online

ACCESS | Metrics & More | Article Recommendations | Supporting Information

ABSTRACT: Cell culture on microcarriers emerges as an alternative of two-dimensional culture to produce large cell doses, which are required for cell-based therapies. Herein, we report a versatile and easy solvent-free greener fabrication process to prepare microcarriers based on a biosourced and compostable polymer. The preparation of the microcarrier core, which is based on poly(L-lactide) crystallization from a polymer blend, allows us to easily tune the density, porosity, and size of the microparticles. A bioadhesive coating based on biopolymers, devoid of animal protein and optimized to improve cell adhesion, is then successfully deposited on the surface of the microcarriers. The ability of these new microcarriers to expand human adipose-derived stromal cells with good yield, in semistatic and dynamic conditions, is demonstrated. Finally, bead-to-bead cell transfer is shown to increase the yield of cell production without having to stop the culture. These microcarriers are therefore a promising and efficient green alternative to currently existing systems.

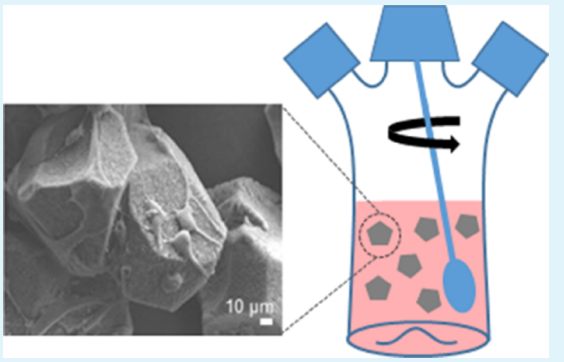

KEYWORDS: *poly(L-lactide), human adipose stromal cell, dynamic culture, spherulite, cell proliferation*

1. INTRODUCTION

Live cell-based therapies are by now well established in modern medicine, and the therapeutic potential of a wide variety of cell types (i.e., fibroblasts, lymphocytes, endothelial cells, pancreatic islets, stem cells) has been successfully demonstrated.[1] However, regardless of the specific application, one major challenge that still impedes the industrial development of cell-based therapies is the large number of cells required to treat a single patient.[2] For example, in the case of human mesenchymal stromal cells (hMSCs), which are considered as especially promising candidates for cell therapy, doses ranging from 100 to 150 million cells per patient are usually required.[3] This highlights the critical need for efficient cell expansion technologies to ensure the full development of cell-based therapies.

The expansion of anchorage-dependent cells usually involves the culture of cells as a monolayer in plastic flasks in static conditions.[4−7] When a large number of cells are not required, this two-dimensional (2D) culture technique offers the advantages of simplicity and easy handling. However, it shows also a series of drawbacks such as the limited possibility to monitor cell growth during the culture and the static nature of the culture, which leads to gradients of pH, dissolved oxygen, and nutrient and metabolite concentrations.[5,6] Moreover, the scalability of this 2D approach to produce a larger number of cells is considerably limited and would generate considerable amounts of nonrecycled waste.

To overcome these limitations of 2D culture, microcarrier (MC) technology was introduced by Van Wezel in 1967. It relies on cell growth on the surface of small solid particles suspended in the growth medium under slow agitation.[8] The main asset of cell culture on MCs is to provide a large solid surface for cell proliferation in a limited volume of the medium while keeping relatively homogeneous and controlled environmental culture conditions.[9] However, dynamic culture using MCs is a complex and multiparameter approach that requires a careful selection of the appropriate MC depending on the type of vessel, stirring regime, and cell type.[10] In this context, a wide variety of MCs with various characteristics have been commercially developed.[11] However, they have been designed with the aim of propagating anchorage-dependent cell lines used in the production of vaccines and biopharmaceuticals and are usually not optimized for cells directly used as therapeutic agents, notably stem cells, which need to be gently harvested after culture. Moreover, they are frequently coated with animal proteins to ensure cell adhesion, which might restrict their

Received: September 18, 2020
Accepted: October 19, 2020

application for therapeutic applications due to safety concerns.[12]

Additionally, techniques often used to fabricate MCs usually generate a lot of waste and do not take into account the requirements of a truly circular economy. For instance, a very popular approach is based on an emulsion solvent evaporation process. Although this technique allows controlling the porosity of the microparticles via the use of effervescent or porogenic additives and, to a lesser extent, to vary their size,[13−15] it is not biocompatible and environmentally friendly since it relies on toxic organic solvents. To overcome this drawback, nonsolvent-based techniques, such as jet milling based on a grinding process[16] and jet break-up solvent displacement,[17] have been developed. However, these methods allowed controlling the MC size but not their morphology, which limits their applications in cell culture.

Recently, we developed in our group an organic solvent-free process to produce microcarriers of tunable size and porosity.[18] This process relies on the spherulitic crystallization of poly(L-lactide) (PLLA), an FDA-approved, biosourced, and industrially compostable polymer, in its miscible blend with poly(ethylene glycol) (PEG). At the end of the process, PEG is dissolved in water to retrieve individual PLLA spherulites (Figure 1A).[18]

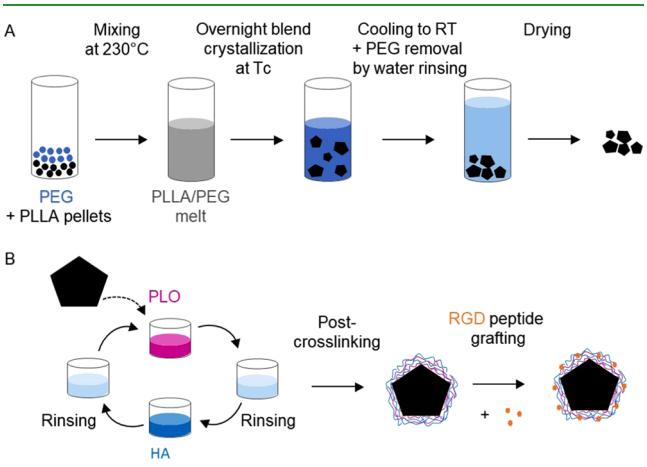

Figure 1. Description of the fabrication process of porous microcarriers via spherulitic crystallization of PLLA (A) and subsequent surface biofunctionalization by layer-by-layer assembly of poly(L-ornithine) (PLO) and hyaluronic acid (HA) followed by post-cross-linking and grafting of a bioadhesive RGD peptide (B).

Herein, we show that the processing parameters used to fabricate such PLLA spherulites can be adapted to the production of MC cores with constant core composition but tunable porosity, size, and density for both semistatic and dynamic cell cultures. Moreover, to improve cell adhesion, the MC surface is subsequently modified with a bioadhesive coating devoid of animal proteins and toxic chemicals. For this, a layer-by-layer (LbL) film composed of biocompatible hyaluronic acid (HA) and poly(L-ornithine) (PLO) is deposited from aqueous solutions on the MC surface and then chemically cross-linked and grafted with an RGD peptide (Figure 1B). Therefore, the whole fabrication process developed to produce MCs for cell culture is fully green and free from toxic chemicals since it requires only biocompatible materials and water. The performance of these surface-functionalized MCs is then demonstrated in both semistatic and dynamic culture conditions (spinner flasks) using human adipose-derived stromal cells (hASCs).

2. RESULTS AND DISCUSSION

2.1. Fabrication, Characterization, and Optimization of Microcarrier Cores. MCs need to meet three stringent specifications to be used as microcarriers for dynamic cell expansion: an optimal size for cell growth and maximization of available surface area, an appropriate sedimentation rate to avoid accumulation at the bottom of the reactor under reasonable stirring rates (i.e., 25−50 rpm),[19] and sufficient mechanical resistance to withstand stirring. For microporous MCs, diameters of 100−230 μm are reported to be the optimal size.[9] This size range results from a compromise between the maximization of the total surface area, the stability of the suspension (both in favor of a smaller size), and a minimal surface area per microcarrier. For dynamic cell expansion, MCs also need to be well suspended in the medium to optimize nutrient and waste-product transfers between cells and the surrounding medium as well as to avoid microcarrier aggregation, which can compromise cell viability.[20] Commercial microporous MCs typically show sedimentation rates between 12 and 19 cm min^{-1}.[21] Finally, MCs need to be able to withstand the mechanical stress induced by the agitation in dynamic conditions as breakage products would be detrimental to the final cell product.[5]

To produce MC cores showing optimal characteristics for dynamic culture, we used a fabrication process based on the PLLA crystallization in a PLLA/PEG blend (Figure 1A), which allows us to tune easily the characteristics of MCs by varying the processing parameters.[18] Briefly, PLLA and PEG pellets are mixed in a given ratio and heated at 230 °C to obtain a homogeneous blend. The resulting melt is subsequently cooled to the crystallization temperature (between 103 and 130 °C) to allow PLLA crystallization. The blend is then cooled to room temperature, and individual spherulites are retrieved following the dissolution of PEG in water. The effects of blend composition, crystallization temperature, and PLLA molar mass on PLLA spherulite characteristics were systematically investigated to provide PLLA core MCs well adapted for dynamic cell expansion in spinner flasks.

2.1.1. Influence of the PLLA/PEG Blend Composition. Younes et al. characterized PLLA/PEG blends made from 10:90 to 90:10 mass ratios. According to their findings, if one component represents more than 20% of the blend, it crystallizes, leading to two partially segregated crystalline phases dispersed in an amorphous matrix. For more dilute compositions, crystallization is possible only for the dominant component, resulting in a noncrystalline matrix composed of the minor component and the noncrystallized fraction of the semicrystalline dominant component.[22] Several authors also reported that a PEG content lower than 10% does not result in crystallization-induced phase separation.[23−25] Based on these observations, theoretical PLLA/PEG blend compositions leading to crystallization-induced phase separation can range from 10:90 to 80:20. The influence of blend composition on spherulite morphology for PLLA/PEG ratios ranging from 10:90 to 30:70 was described by Kuterbekov et al.[18] They reported that a higher PLLA content led to denser spherulites with smaller pores. However, they did not investigate the properties of these MCs in aqueous solutions.

Scanning electron microscopy (SEM) images of spherulites prepared at a crystallization temperature of 110 °C from

https://dx.doi.org/10.1021/acsami.0c16875
ACS Appl. Mater. Interfaces XXXX, XXX, XXX−XXX

different PLLA/PEG ratios (using a PLLA of a lower molar mass 20 000 g mol^{-1}, hereafter called PLLA20), including much higher PLLA concentrations than reported by Kuterbekov et al., are shown in Figure 2. As expected, a

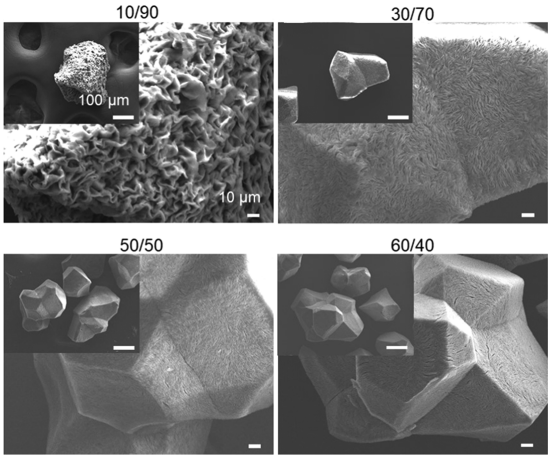

Figure 2. SEM images illustrating the influence of the PLLA20/PEG ratio on MC morphology. The microcarriers were obtained at a crystallization temperature of 110 °C. The scale bars are identical in the four panels.

higher PLLA content leads to denser MCs showing a reduced pore size but also to MCs presenting a better-defined shape with an increasing number of facets as the PLLA content increases. This polyhedral shape results from the impingement of adjacent spherulites due to the competing spherulitic growth inside the blend.[26] By changing the blend composition, it is thus possible to obtain a variety of morphologies ranging from irregularly shaped and highly porous spherulites to denser and well-faceted spherulites. While less dense spherulites could have an appropriate sedimentation rate for dynamic culture applications, they may lack the mechanical resistance required to withstand the agitation necessary to dynamic cell culture.

2.1.2. Influence of the Crystallization Temperature. It is well known that crystallization temperature influences the spherulite size due to the strong temperature dependence of the spherulite nucleation process, with lower temperatures leading to smaller spherulites[18] and higher temperatures corresponding to less numerous nucleation seeds and therefore larger spherulites.[18] The inspection of SEM images of spherulites prepared from a 20:80 PLLA20/PEG ratio using different crystallization temperatures of 103, 110, 120, and 130 °C (as well as a boxplot with quantitative measurements of the spherulite size) indeed showed that the higher the crystallization temperature, the larger the size of the MCs, as expected (Figure 3). Notably, by selecting the crystallization temperature in a range narrower than 30 °C, the average spherulite size can be varied by a factor as large as four, showing the considerable versatility of the fabrication process. We noticed also that the MC morphology remained very similar for the different tested crystallization temperatures, demonstrating that this parameter does not affect the MC microstructure.

2.1.3. Influence of the PLLA Molar Mass. The influence of the PLLA molar mass on spherulite morphology was also investigated using two PLLA samples of 20 000 (PLLA20) and 40 000−70 000 g mol^{-1} (PLLA40), respectively, whereas the PEG molar mass, the composition of the PLLA/PEG blend

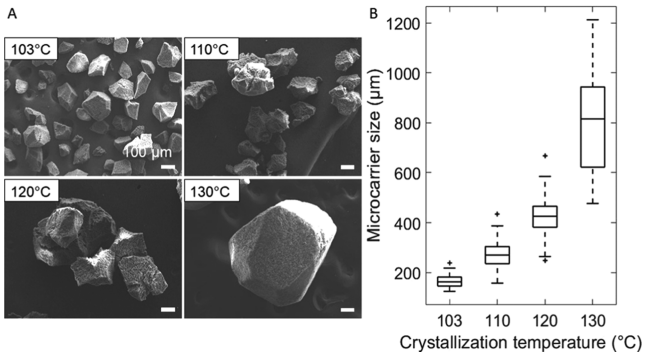

Figure 3. (A) SEM images of PLLA20 MCs prepared with a PLLA20/PEG ratio of 20:80 at different crystallization temperatures. The scale bars are identical in all panels. (B) Boxplot showing the variation of the PLLA20 MC size versus crystallization temperature.

(50:50), and the crystallization temperature (110 °C) were kept constant at their finally selected values (see below). The morphology of MCs observed by SEM was very similar whatever the PLLA molar mass, showing multiple faceted particles of similar porosity (Figure 4A). Moreover, an increase of PLLA molar mass led to a slight decrease of MC size (Figure 4B).

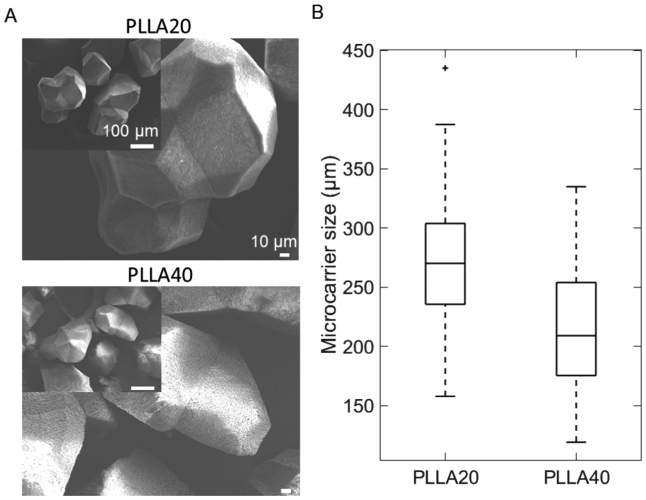

Figure 4. SEM images (A) and size (B) of MCs prepared at a crystallization temperature of 110 °C using the same PLLA/PEG ratio (50:50) but different PLLA molar masses (i.e., PLLA20 and PLLA40). The scale bars are identical in all panels.

2.1.4. Microcarrier Optimization for Dynamic Culture. The sedimentation rate depends not only on the medium density and viscosity but also on the MC density, size, shape, and porosity. As the density of PLLA is reported to be 1.24 g cm^{-3}[27] and the MC shape is defined by the crystallization process, the only parameters that can be modified to tune the sedimentation rate are the MC porosity and size. The MC porosity can be modulated by changing the PLLA/PEG ratio, and the MC size depends on the crystallization temperature and, to a much lesser extent, on PLLA molar mass, as described above.

Suspension and mechanical resistance under agitation (40 rpm) of PLLA20 MCs produced at different crystallization temperatures (from 110 to 130 °C) and with blends of different PLLA20/PEG ratios (20:80, 30:70, 50:50, and 70:30)

https://dx.doi.org/10.1021/acsami.0c16875
ACS Appl. Mater. Interfaces XXXX, XXX, XXX−XXX

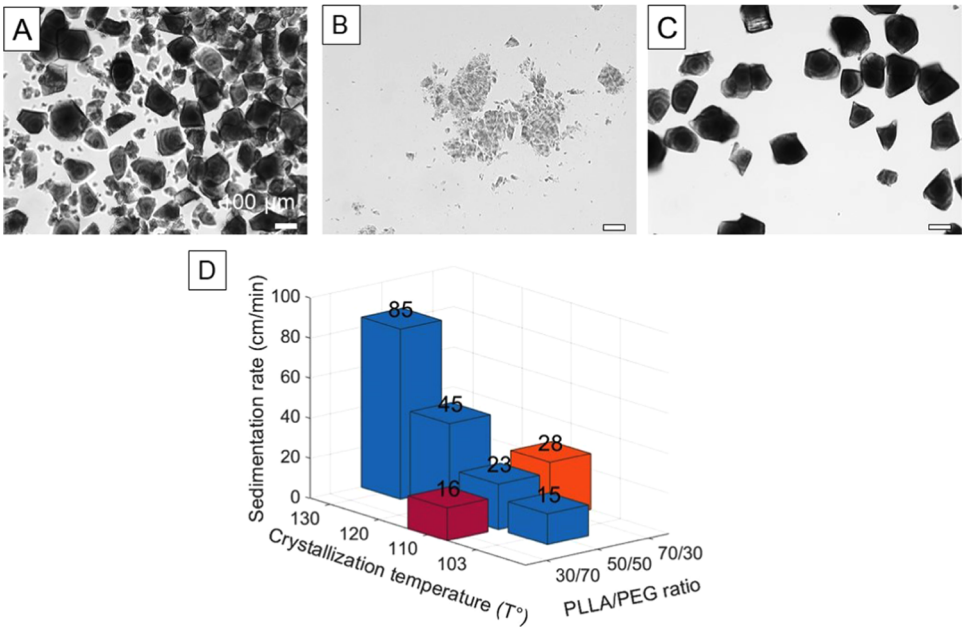

Figure 5. (Top) optical microscopy images of MCs prepared from (A) a 50:50 PLLA20/PEG blend crystallized at 110 °C and stirred for 2 days, (B) a 30:70 PLLA40/PEG blend crystallized at 110 °C and stirred for 4 days, and (C) a 50:50 PLLA40/PEG blend crystallized at 110 °C and stirred for 7 days; the stirring was performed in a spinner flask at 40 rpm. The scale bars are identical in all images. (Bottom) Variation of the sedimentation rate of PLLA40 MCs measured in water as a function of the processing parameters used for their fabrication, i.e., crystallization temperature and PLLA40/PEG ratio.

were first tested in spinner flasks to select the optimal MC cores for dynamic cell culture. Some of these PLLA20 MCs suspended well in an aqueous solution under slow agitation (40 rpm). However, their mechanical resistance was limited as they broke after only 2 days of agitation (Figure 5A). To overcome this problem, PLLA40 cores prepared with a PLLA sample of a higher molar mass were investigated. Indeed, higher molar masses are expected to result in an increased proportion of tie molecules bridging different lamellar crystals within the spherulites, which should contribute to reinforcing their mechanical resistance. The sedimentation rates of such MCs prepared from different PLLA40/PEG ratios (30:70, 50:50, and 70:30) and at different crystallization temperatures (103, 110, 120, and 130 °C) were first measured in an aqueous solution (Figure 5D). Commercial microporous MCs typically show sedimentation rates between 12 and 19 cm min^{-1}.[21] The values obtained here varied between 15 and 85 cm min^{-1} (Figure 5D), with the MCs obtained either from a 30:70 ratio crystallized at 110 °C or from a 50:50 ratio crystallized at 110 or 103 °C being close to this requirement. Other MCs had a higher sedimentation rate due to their larger size or smaller porosity. Crucially, MCs prepared from a 50:50 ratio at 110 and 103 °C (Figure 5C) were significantly more mechanically resistant than the ones prepared from a 30:70 ratio (Figure 5B), as they did not break even after 7 days of stirring in the aqueous solution. Diameter measurements performed by optical microscopy on 50:50 MCs prepared at 110 °C provided values of 220 ± 56 and 217 ± 45 μm before and after 7 day stirring at 40 rpm, respectively, confirming that microcarriers are not broken under stirring. Therefore, PLLA40 prepared with a 50:50 ratio and crystallization temperatures of 103 and 110 °C were selected for the cell culture assays. The average sizes of these MCs were 132 ± 23 and 220 ± 56 μm, respectively (Figure S1).

2.2. Bioadhesive Coating Fabrication and Characterization. A (PLO/HA) LbL coating was deposited on the MC surface to promote cell adhesion. Coatings based on these polymers showed good results for a variety of cell culture applications,[28−31] and this specific polyelectrolyte association was previously successfully deposited on microparticles used as a scaffold for bone regeneration.[32] This (PLO/HA) film was subsequently cross-linked using a biocompatible cross-linking reaction based on carbodiimide chemistry to improve the stability and the mechanical properties of the coating toward stem cells.[33−35] Then, a bioadhesive RGD peptide was grafted on the cross-linked LbL to increase cell adhesion, challenged by the shear stress occurring in dynamic culture conditions.[20] The overall strategy is illustrated in Figure 1B.

The variation of the thickness of dry (PLO/HA) film as a function of the number of deposited (PLO/HA) bilayers was investigated on planar model surfaces (Figure S2A). It was previously demonstrated that eight bilayers were sufficient to obtain a homogeneous film in a similar system.[36] MCs coated with eight (PLO/HA) bilayers were thus dipped in a rhodamine solution to visualize the film distribution on MCs. This allowed confirming that MCs were uniformly covered by the LbL film (Figure S2B). Therefore, such a coating with $(PLO/HA)_8$ was used to modify the MC surface. This LbL coating was subsequently grafted with an RGD peptide, and two RGD concentrations (1 and 0.1 mM) were tested to optimize cell adhesion and proliferation on MCs. Indeed, as of now, no consensus has been reached on the optimal RGD concentration. While a higher RGD surface density is usually related to cell spreading, survival, and proliferation,[37] it has also been reported that a large adhesion strength tends to reduce cell migration/proliferation and induce cell differentiation instead.[38]

The grafting of RGD peptide on $(PLO/HA)_8$ films deposited on planar surfaces was first investigated by using a

https://dx.doi.org/10.1021/acsami.0c16875
ACS Appl. Mater. Interfaces XXXX, XXX, XXX−XXX

fluorescent RGD-FITC peptide at two concentrations following an *N*-hydroxysulfosuccinimide (sulfo-NHS)/*N*-(3-dimethylaminopropyl)-*N*′-ethylcarbodiimide hydrochloride (EDC) activation step. A control sample prepared without the activation step was also produced. Imaging by epifluorescence microscopy of the samples grafted using 1 and 0.1 mM RGD (Figure 6A,B, respectively) revealed the successful

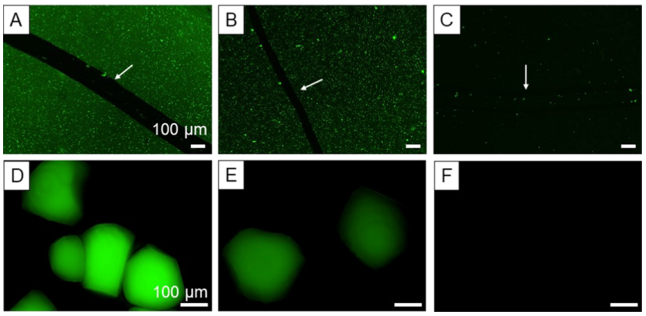

Figure 6. Fluorescence microscopy images of $(PLO/HA)_8$ bilayer films deposited on flat model surfaces activated by sulfo-NHS/EDC and incubated in (A) 1 mM or (B) 0.1 mM RGD-FITC solution and (C) control without any prior activation incubated in a 0.1 mM RGD-FITC solution. Deliberate scratches (see white arrows) were made on the films to visualize the fluorescence background. Fluorescence microscopy images of MCs coated with eight (PLO/HA) bilayer films activated and incubated in (D) 1 mM or (E) 0.1 mM RGD-FITC peptide solution and (F) control without any prior activation then incubated in 0.1 mM RGD-FITC solution. The scale bars are identical in each line.

grafting of the peptide. As seen from the difference of fluorescence intensity between those two images, the higher the peptide concentration used for the grafting, the higher the fluorescence intensity on the film, which means a higher degree of peptide grafting (qualitative evaluation). Moreover, the chemical grafting of the peptide on the $(PLO/HA)_8$ films required the activation of the carboxylic groups present on HA chains. Indeed, when the activation step was omitted (Figure 6C), the peptide was simply slightly adsorbed on the film and rinsed away in subsequent steps, as evidenced by the much lower fluorescence intensity. Similar experiments were performed to evaluate the grafting of the peptide on $(PLO/HA)_8$-modified MCs (Figure 6D−F), confirming that the activation step is required to chemically graft the peptide on the film and that a higher peptide concentration led to a larger amount of peptide grafted on the film.

2.3. Cell Culture on Microcarriers. *2.3.1. Culture in Semistatic Conditions.* hASCs were selected to assess the MC performance for cell expansion as they are replacing bone-derived MSCs as the gold standard for MSC-based therapy.[39,40] As the MCs presented here are novel, no information on how they would interact with cells is available. Thus, their ability to support hASC adhesion and proliferation was first evaluated in semistatic conditions. The objective was also to select the most efficient surface modification and then test the same parameters in dynamic conditions.

To perform assays in semistatic conditions, intermittent agitation was only carried out during the adhesion step and then the rest of the culture was done in static conditions. PLLA cores prepared from a PLLA40/PEG ratio of 50:50 crystallized at 110 °C were used for these studies. These PLLA cores were coated with a film of cross-linked LbL grafted with RGD (0.1 and 1 mM, referred to as MC-RGD 0.1 and MC-RGD 1, respectively). Bare MCs and MCs coated with cross-linked LbL (referred to as MC-LbL) were used as controls. Cell proliferation was followed over time (up to 5 days).

The initial cell adhesion was quantified 4 h after seeding on MCs in semistatic conditions (intermittent agitation) by measuring their metabolic activity. hASCs were able to attach and grow on MCs whatever the surface treatment, but adhesion and proliferation were higher when the MCs were grafted with RGD (Figure 7A). Coating the surface of MCs

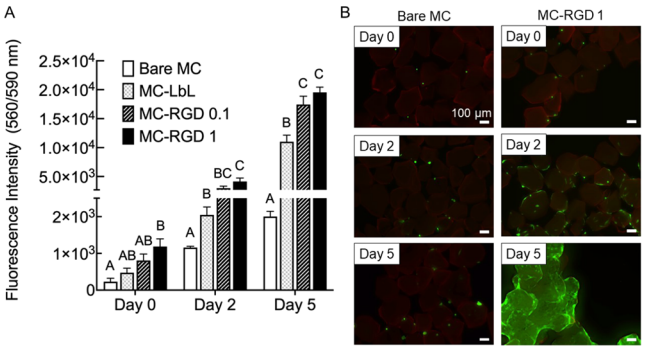

Figure 7. hASC proliferation performed in semistatic conditions on different MCs: (A) Metabolic activity evolution (PrestoBlue) of cells grown on bare MCs, MC coated with cross-linked LbL (MC-LbL) and MCs coated with cross-linked LbL grafted with 0.1 mM (MC-RGD 0.1) and 1 mM RGD (MC-RGD 1) over 5 days ($N = 2$, $n = 3$). Bars topped with different letters indicate a significant difference ($p < 0.05$). (B) Live/dead images of bare MCs and MC-RGD 1 on days 0, 2, and 5. The scale bars are identical in all panels.

with cross-linked LbL increased cell proliferation but not initial cell adhesion. Only MC-RGD 1 allowed a higher cell attachment than the bare MCs. Overtime, hASC proliferation was higher on RGD-coated MCs, but no significant difference was observed between the two concentrations of RGD. This observation was confirmed by live/dead assays (Figure 7B). Cells reached confluency on MC-RGD 1 after 5 days when almost no cells were visible on the bare MCs. The absence of PI (red) staining indicated the lack of major cytotoxicity of the MCs, whatever their surface treatment.

DNA content quantification was also performed to measure cell proliferation. However, the kit reagents interacted with MCs whatever the experimental settings, precluding any accurate quantification (data not shown).

Cell adhesion and viability on MC-RGD-1 with different core morphologies (obtained from MCs prepared from 30:70, 50:50, and 70:30 PLLA40/PEG blends) were also investigated (Figure S3). No difference could be observed between MCs prepared from 30:70 and 50:50 PLLA40/PEG ratios, while a lower cell adhesion was found on MCs prepared from a 70:30 PLLA40/PEG ratio, indicating that cell adhesion is influenced by the MC surface morphology underneath the coating.

2.3.2. Culture in Dynamic Conditions. For the dynamic culture, PLLA cores prepared with a 50:50 PLLA40/PEG ratio crystallized at 103 °C were used. These PLLA cores showed the same morphology and porosity as the ones used for semi-static studies (Figure S4) but could be suspended better under gentle agitation, thanks to their lower average size (Figure S1). Similarly to the MCs used for semi-static culture, these PLLA cores were coated with LbL and grafted using 1 mM peptide (MC-RGD 1). Indeed, preliminary assays performed on bare

https://dx.doi.org/10.1021/acsami.0c16875
ACS Appl. Mater. Interfaces XXXX, XXX, XXX−XXX

MCs and MCs coated with LbL only, confirming that cell adhesion was not high enough on these MCs to perform cell culture in dynamic conditions (Figure S5). An agitation speed of 45 rpm was selected as the best compromise between maintaining the MCs in suspension in the spinner flask and keeping cells on the MCs (data not shown).

Very little to no toxicity was observed when hASCs were grown on MC-RGD 1, even after 7 days of culture (Figure 8A–C). Cells were metabolically active and continued to

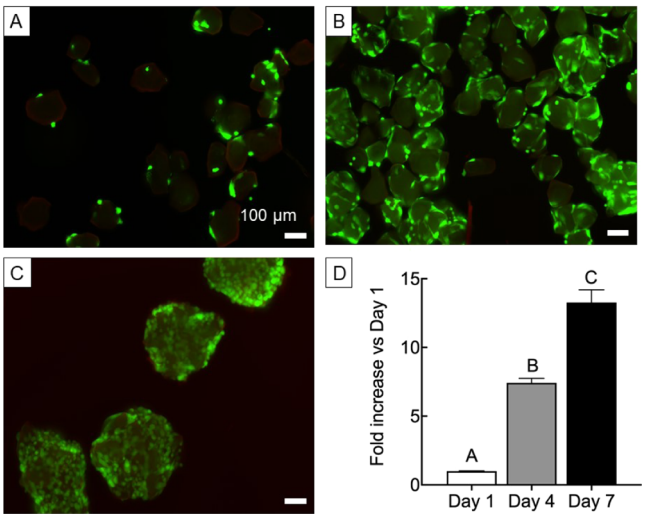

Figure 8. Viability and proliferation of hASCs grown on MC-RGD 1 in dynamic conditions: analysis of hASC viability by live/dead staining on (A) day 1, (B) day 4, and (C) day 7. The scale bars are identical in all panels. (D) Quantification of cellular metabolic activity (measured with PrestoBlue). Bars topped with different letters indicate a significant difference ($p < 0.05$) ($N = 3$, $n = 3$).

proliferate over time (Figure 8D). The number of cells on MCs increased by 7.42 ± 0.97-fold between day 1 and day 4 and up to 13.27 ± 2.27-fold between day 1 and day 7 to reach confluency.

Slight MC aggregation was observed by day 7 due to cell–cell adhesion between MCs (Figure 8C). MC aggregate formation was also reported for culture performed on commercial Cytodex MCs, which caused mass-transfer limitations, forming stagnant cores and leading to cell necrosis.[41−43] However, in our study, the MC aggregates were small-sized (250–400 μm) and did not cause cell death.

To compare the performance of PLLA MCs with commercial ones, dynamic culture assays were also performed using Cytodex 3 microcarriers (Figure S6). The final fold increase obtained with these MCs was 22 ± 1.49 by day 7 of culture, which is comparable to the one measured for PLLA MCs, albeit slightly higher.

The morphology and cytoskeletal organization of hASCs grown on the MC-RGD 1 surface were studied by staining of the cell cytoskeleton at different time points. The cell nucleus was simultaneously counterstained with 4′,4′,6-diamidine-2′-phenylindole dihydrochloride (DAPI; Figure 9A). Layer-by-layer Z stacking and 3D reconstruction from the confocal laser scanning microscopy (CLSM) images showed that cells exhibited prominent actin fibers on the MC surface as early as on day 1 after seeding. By day 4, the cells spread on the MC surface with well-defined actin filaments, which progressively

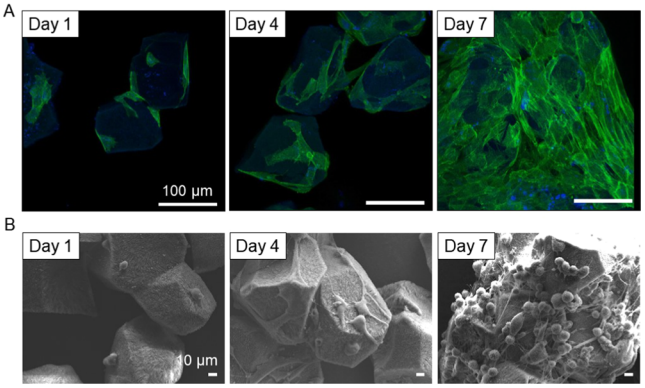

Figure 9. Cytoskeletal organization and spreading of hASCs grown on MC-RGD 1 surface: (A) CLSM micrographs of F-actin-stained hASCs. Phalloidin stains actin filaments (green) and DAPI stains cell nuclei (blue). The blue color observed on the MC surface on day 1 and day 4 results from the interaction between DAPI and the bioadhesive coating deposited on the MC surface. (B) SEM images of hASCs grown on MC-RGD 1.

increased with culture duration and covered the entire surface of the microcarriers by day 7.

Additionally, SEM analysis was conducted at the same time points to characterize cell morphology on MCs. On day 1, the cells appeared rounded on the carriers (Figure 9B). However, on day 4 after seeding, cells flattened and appeared well spread on the MC surface. On day 7, the cells underwent active proliferation and formed several cell bridges with the adjacent MCs to form aggregates (Figure 9B).

Several studies describing mesenchymal stromal cell expansion on various commercial microcarriers are available in the literature. Eibes et al. cultured MSCs on Cultispher-S microcarriers in a spinner flask and obtained an 8.4-fold increase in the cell number on day 8.[44] A fourfold increase in the growth rate of hMSCs was reported on Cytodex1 microcarriers on day 7 of spinner flask culture by Schop et al.[45] Similarly, a 13.6-fold expansion on Cytodex 3 microcarriers was reported on day 11.[46] Even though a direct comparison with these earlier reports may not be accurate due to variations in cell type, cell source, methodology for cell characterization, culture medium, and culture duration, it can be stated that the MCs developed in our study allowed a significantly high cell proliferation rates in dynamic culture over a short duration of 7 days.

2.3.3. Cell Proliferation by Bead-to-Bead Transfer. One advantage of dynamic culture on MCs is the possibility to increase the yield of cells at the end of the production period by the addition of fresh MCs during the proliferation phase to perform what is called "bead-to-bead transfer". This offers new surfaces to the cells to attach and proliferate.

New MC-RGD 1 particles were introduced into the spinner flasks at a ratio of 0.5:1 (new MCs/initial MCs), 5 days after initial seeding. To discriminate the fresh MCs from the initial ones, the coating of fresh MCs was labeled with poly(allylamine)–rhodamine (Figure 10A). The culture was maintained at an intermittent mode of agitation for 12 h (i.e., agitated for 2 min and then kept static for 28 min). Maintaining an intermittent agitation[47] allowed the MCs to be in close proximity with one another, which enabled the transfer of cells from initial MCs to the new MCs.[48] It was observed that cell transfer started as early as 1 h after the addition of fresh MCs.

https://dx.doi.org/10.1021/acsami.0c16875
ACS Appl. Mater. Interfaces XXXX, XXX, XXX–XXX

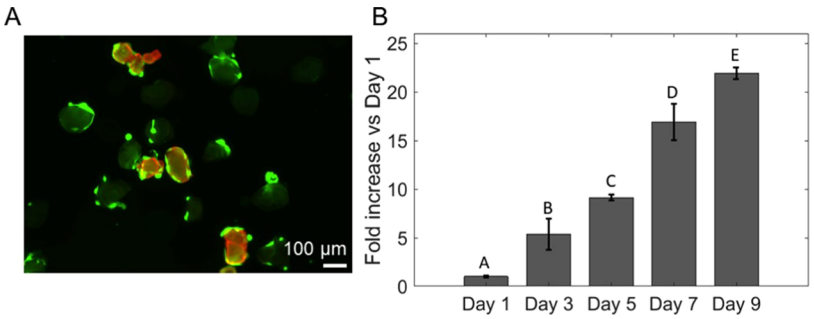

Figure 10. Bead-to-bead cell-transfer assay performed with hASCs cultured on MC-RGD 1. In total, 50% of fresh MC-RGD 1 (stained in red with poly(allylamine)−rhodamine) were added to the existing culture after 5 days of cell expansion. (A) Live/dead images after 12 h of intermittent agitation. Cells were stained with calcein-AM. (B) Quantification of cellular metabolic activity (PrestoBlue) (N = 1, n = 3). Bars topped with different letters indicate a significant difference ($p < 0.05$).

The transfer of cells from the initial microcarriers to the new ones added during the culture can be explained by two possible mechanisms. The first one is related to the attachment of free-floating cells in the medium. Indeed, cells can detach from the confluent microcarriers and then colonize the new MCs. Verbruggen et al. attributed the high increase in the cell number after the addition of fresh beads in the medium to this mechanism, rather than to the increased proliferation rates.[49] According to the second mechanism, cells attached to initial MCs migrate on the new ones thanks to the formation of cellular bridges between both MCs during the intermittent agitation performed just after the addition of the new MCs in the medium.[50] According to the microscopy images recorded just after the intermittent agitation step (Figure 10A) and the fact that we observed only a very few free-floating cells in our cultures, we assume that the second mechanism of cell transfer was achieved during our bead-to-bead cell transfer assays.

Quantification of cell proliferation by evaluation of cell metabolic activity was performed during the culture (Figure 10B). Values of 16.89 ± 1.8- and 21.87 ± 0.6-fold increase were measured on day 7 and day 9, respectively, proving the advantage of bead-to-bead cell transfer to improve the cell yield.

After the MCs reach confluency, a portion can be extracted from the culture system and fresh empty MC can be added instead to provide the additional surface area for cells to attach and continue the proliferation.[51] Routine and extensive subculturing of cells has shown to induce cells into replicative senescence, a state of growth arrest.[52] Bead-to-bead methodology of cell transfer does not require intermediate passaging of cells and therefore provides opportunities for cell expansion with minimum manipulation. In this study, we give direct evidence that hASCs display bead-to-bead transfer on the PLLA MCs. Therefore, this methodology offers a cost-effective alternative to scale up the commercial production of stem cells.

2.4. Magnetic Microcarriers. After the expansion step on MCs, the cells usually need to be detached and separated from MCs.[6] As of now, the separation step has received little attention and usually involves the use of filtration or centrifugation.[53] Alternatively, MCs displaying magnetic properties could facilitate MC handling during MC−cell separation by allowing to immobilize MCs using a magnet. This feature could also ease MC handling during culture, such as for medium replenishment. To test the fabrication of magnetic PLLA MCs, magnetic nanoparticles (MNPs) were incorporated into the PEG powder used for the preparation of PLLA/PEG (Figure 1A). The obtained MCs displayed a superparamagnetic behaviour (Figure S7A) and could simply be attracted in a solution using a 1.4 T magnet (Figure S7B). The release of iron in solution was measured after a storage time of several weeks and was found negligible (data not shown), evidencing the stability of these MCs. Additionally, these magnetic MCs supported cell adhesion and proliferation to the same extent as nonmagnetic MCs (results not shown). These experiments contribute to demonstrate the versatility of our fabrication process to produce MCs with a large range of characteristics.

3. CONCLUSIONS

We have disclosed the preparation of biodegradable MCs composed of a biosourced and nonexpensive polymer, easy to produce with a scalable solvent-free process, which could even be industrially composted after use for optimal circularity. Their preparation process is extremely versatile, and the MC size, porosity, and mechanical resistance can easily be optimized by tweaking trivial processing parameters such as crystallization temperature and PEG content, without impacting the global process. Additionally, the MC surface can be easily functionalized with an animal protein-free bioadhesive polysaccharide/polypeptide coating, which constitutes a supplementary asset with respect to current regulations; this coating is subsequently grafted with an RGD peptide for optimal cell adhesion.

The PLLA MCs support growth and proliferation of stem cells in semi-static conditions and, most importantly, in dynamic conditions too. hASCs can be easily expanded (more than by 12-fold over 1 week) and the cell production yield can be increased by successful bead-to-bead cell transfer. Cell retrieval and separation from the MCs can even be facilitated by providing them with magnetic properties. Alternatively, as they are composed of biocompatible FDA-approved components and are animal- and organic-solvent-free, directly implanting the cell−MC complexes may be considered in the future, provided that in vivo studies demonstrate no toxicity. Therefore, our new MCs are a promising animal protein-free greener alternative to commercial MCs used for stem cell expansion and tissue engineering alike.

4. EXPERIMENTAL SECTION

4.1. Materials. PLLA20 (20 000 g mol^{-1}, $Đ$ 1.1) and PEG (3500 g mol^{-1}) were obtained from Sigma-Aldrich. PLLA40 (M_n 40 000−70 000 g mol^{-1}) was obtained from Polysciences. Dextran-coated iron oxide magnetic nanoparticles (MNPs) were purchased from Ocean

https://dx.doi.org/10.1021/acsami.0c16875
ACS Appl. Mater. Interfaces XXXX, XXX, XXX−XXX

Nanotech. Sodium hyaluronate (HA) (360 000 g mol^{-1}) was obtained from Lifecore Biomedical. Poly-L-ornithine hydrobromide (PLO) (78 000 g mol^{-1}) was purchased from Alamanda Polymers. Rhodamine-labeled poly(allylamine) (M_w 15 000 g mol^{-1}) was purchased from Surflay Nanotec GmbH. Poly(ethyleneimine) (PEI) (M_n 60 000 g mol^{-1}), *N*-hydroxysulfosuccinimide sodium salt (Sulfo-NHS) (98%), *N*-(3-dimethylaminopropyl)-*N*′-ethylcarbodiimide hydrochloride (EDC) (98%), 4-(2-hydroxyethyl)piperazine-1-ethanesulfonic acid (HEPES) (99.5%), sodium chloride (NaCl) (99.5%), dimethylsulfoxide (DMSO), and hexamethyldisilazane (HMDS) (99%) were bought from Sigma-Aldrich. 2-(*N*-morpholino)-ethanesulfonic acid (MES) (99%) and absolute ethanol (95%) were obtained from Acros. GRGDS peptide (RGD peptide) (98%) and fluorescent RGDK-FITC (95%) were provided by Genecust. Milli-Q grade water (resistivity of 18.2 × 10^6 Ω m) was produced by a Milli-QReference system of Merck Millipore. Mesenchymal stem cell growth medium 2 (basal medium supplemented with supplement mix) was purchased from Promocell. Dulbecco's phosphate-buffered saline devoid of calcium and magnesium (DPBS), StemPro Accutase Cell Dissociation Reagent, Alexa Fluor 488 phalloidine, calcein-AM, and PrestoBlue Cell Viability reagent were provided by ThermoFisher Scientific. Penicillin/streptomycin (PEST) was obtained from Life Technologies. Triton TM X-100, bovine serum albumin (96%) (BSA), glutaraldehyde aqueous solution (25%), and 4′,4′,6-diamidine-2′-phenylindole dihydrochloride (DAPI) (98%) were purchased from Sigma-Aldrich. Corning Costar Ultra-Low Attachment Multiple Well Plates were purchased from VWR. Cellstar 24-well cell culture plates were purchased from Greiner Bio-One. Spinner flasks of 125 mL capacity equipped with a magnetic ball impellor (Magna-Flex, Wheaton) were used to perform cell culture in dynamic conditions. Single-side-polished (100) silicon wafers were purchased from TOPSIL. Cytodex 3 microcarriers were obtained from GE Healthcare. Ethidium bromide was purchased from Biotium. Human adipose-derived stromal cells (hASCs) were collected from lipoaspirates harvested from one adult donor, who had provided their informed consent.

4.2. Fabrication of Microcarriers. PLLA microcarriers were prepared via isothermal spherulitic crystallization of PLLA/PEG blends, as described in Figure 1A. PLLA of two different molar masses (PLLA20 and PLLA40) were used. PLLA and PEG in the form of dry powders were first combined with the desired PLLA/PEG ratio (ranging from 10:90 to 70:30) and melt-mixed at 230 °C for 5 min under dry argon, followed by vortexing to obtain a homogeneous melt. The melt was then isothermally crystallized overnight under an inert atmosphere in a glass tube fitted with a rubber septum at a given temperature (comprised between 103 ± 0.1 and 130 ± 0.1 °C) fixed by a heated oil bath. After crystallization, the blend was cooled down to room temperature and then repeatedly washed with Milli-Q water to remove PEG and collect the insoluble PLLA microcarriers.

4.3. Surface Biofunctionalization of Microcarriers. The (PLO/HA) films were deposited onto the MC surface by the LbL deposition technique.[54] An anchoring PEI layer was deposited as a first layer. PLO and HA dissolved in 0.15 M NaCl (pH 7.4) at concentrations of 0.5 and 1 mg mL^{-1}, respectively, were adsorbed alternately on MCs by immersing the sample for 5 min in the polyelectrolyte solutions. Then, three washing steps were performed in 0.15 M NaCl (pH 7.4), consisting, respectively, of 1 s dipping for ten times, 5 s dipping for five times, and 10 s dipping for one time. The resulting films are denoted $(PLO/HA)_n$, where *n* is the number of (PLO/HA) deposited bilayers. The (PLO/HA) films were also built onto silicon wafers used as model surfaces. For this, silicon wafers were first cleaned by immersion in a freshly prepared piranha mixture [H_2O_2 (35%)/H_2SO_4 (98%) (1:1 v/v)] for 20 min, rinsed extensively with Milli-Q water, and dried under an argon stream. The LbL films were deposited on the samples using an automated dipping machine (Riegler and Kirstein GmbH). For LbL deposition on MCs, wet MCs were placed in porous cell culture inserts (Corning Netwell, 74-μm mesh size) that were fixed on the arm of the dipping robot. After LbL deposition, the (PLO/HA) films were cross-linked through an overnight incubation at 4 °C in a freshly prepared cross-linking solution containing 70 mg mL^{-1} EDC and 11 mg mL^{-1} sulfo-NHS in 0.15 M NaCl (pH 5.5).[33] Then, the samples were rinsed five times for 20 min in HEPES (20 mM in NaCl 0.15 M, pH 7.4) buffer.

The bioadhesive GRGDS peptide was grafted on the cross-linked (PLO/HA) films using the same EDC/sulfo-NHS chemistry as for the cross-linking step. Briefly, MCs or silicon wafers covered by a cross-linked (PLO/HA) film were incubated for 15 min at 4 °C in a freshly prepared 0.1 M MES solution (pH 6.5) containing 70 mg mL^{-1} EDC and 11 mg mL^{-1} sulfo-NHS. Samples were then rinsed thoroughly with the MES solution before being incubated overnight at 4 °C in the peptide solution at a concentration of 0.1 or 1 mM in the MES buffer. Following the grafting, flat samples were rinsed eight times for 20 min in HEPES (20 mM in NaCl 0.15 M, pH 7.4) buffer, thrice for 20 min in ethanol/Milli-Q (50:50 v/v) solution, and twice for 20 min in Milli-Q water to completely remove the non-grafted peptide. For MCs, an additional overnight wash in HEPES was performed before the ethanol/Milli-Q washing step to ensure complete removal of the nongrafted peptide. The same conditions were used to graft fluorescent RGDK-FITC peptide on crosslinked (PLO/HA) films. Control samples were also prepared by omitting the EDC/sulfo-NHS activation step prior to incubation in the peptide solution. MCs grafted with 0.1 and 1 mM peptide concentrations are denoted MC-RGD 0.1 and MC-RGD 1, respectively. The fluorescent MCs were fabricated in a similar manner except that PAH-rhodamine was deposited as the first layer during the LbL process.

4.4. Morphology and Structure of Microcarriers. MCs dried overnight at room temperature and then sputter-coated with an 8 nm thick layer of chromium under high vacuum were observed by scanning electron microscopy (SEM) using a JEOL 7600F scanning electron microscope operated at an acceleration voltage of 15 kV.

4.5. Measurement of the Microcarrier Size. MCs suspended in water were imaged by bright-field microscopy using an Olympus epifluorescence IX71 microscope. The MC average size was obtained as the geometric average between the longest and shortest dimension of 50 randomly selected MCs, as measured using the microscope software (CellSensDimension).

4.6. Sedimentation Rate Estimation. Wet MCs prepared at different crystallization temperatures and PLLA40/PEG ratios were deposited on the top surface of a water column. The time needed for them to sink over 20 cm was recorded five times, with t_0 and t_f being the times for the first and last MCs, respectively, to cover a fixed distance of 20 cm. For each condition, the sedimentation rate was estimated as the median of t_0 and t_f.

4.7. Qualitative Observation of Microcarrier Mechanical Resistance under Stirring. To qualitatively assess the resistance of MCs prepared using different processing parameters to dynamic culture conditions, 50 mL of MC suspension (1 mg mL^{-1}) was placed in a spinner flask under agitation at 40 rpm for up to 7 days. MCs were then observed by bright-field microscopy.

4.8. Determination of the LbL Coating Thickness. The thickness of $(PLO/HA)_n$ with *n* varying from 2 to 10, deposited on flat silicon wafers, then cross-linked, and dried, was measured by ellipsometry using an Accurion EP4 single-wavelength ellipsometer. The wavelength of the laser was 658 nm, and the incidence angle ranged from 60 to 80° (2° increment). The film thickness was determined by fitting a one-layer model with built-in software. The refractive index of the (PLO/HA) film was fixed at 1.5 and that of the silicon substrate to the value tabulated by the manufacturer.

4.9. Visualization of the LbL Coating onto Microcarriers. MCs coated with a (PLO/HA) film were dipped in a rhodamine aqueous solution and then imaged with a Zeiss LSM 700 confocal laser scanning microscope to visualize the coverage of the microcarrier surface by the polyelectrolyte coating.

4.10. Evidence for the Peptide Grafting on LbL Coatings by Epifluorescence Microscopy. The grafting of the RGDK-FITC peptide on both flat model films and surface-modified MCs was evidenced by imaging the samples with an Olympus epifluorescence IX71 microscope equipped with a blue filter U-MNUA2 (excitation 360−370 nm and emission 420−460 nm), a green filter U-MWIBA3 (excitation 460−495 nm and emission 510−550 nm), and a red filter

https://dx.doi.org/10.1021/acsami.0c16875
ACS Appl. Mater. Interfaces XXXX, XXX, XXX−XXX

U-MNIGA3 (excitation 540−550 nm and emission 575−625 nm). The UV light was provided by an X-Cite module, series 120PCQ, from Lumen Dynamics. On flat surfaces, a deliberate scratch was made to evaluate the background fluorescence. The fluorescence intensity of the samples was estimated by comparing the fluorescence intensity measured on the scratch and on the rest of the sample surface.

4.11. MC Preparation for Cell Culture Assays. MCs were first rinsed in ethanol 70% then transferred in sterile DPBS. They were subsequently sterilized by exposure to UV light for 30 min either in well plates or Petri dishes depending on the treated quantity. Following sterilization, the MCs were transferred in the appropriate culture vessels (well plate or spinner flask), the supernatant was removed, replaced by cell culture medium, and conditioned in an incubator for 30 min.

4.12. Routine Culture of hASCs. hASC cells were routinely cultured in cell culture flasks in reconstituted Mesenchymal Stem Cell Growth Medium 2 from PromoCell supplemented with 1% (v/v) PEST in an incubator (Binder CB170 E7) at 37 °C and 5% CO_2. The supplemented culture medium was renewed three times per week, and confluent cells were subcultured using Accutase. Cells were used from passage 4 to passage 8.

4.13. Cell Culture in Semistatic Conditions. On day 0 of the experiments, four types of MC samples prepared from a PLLA40/PEG ratio of 50:50, were placed in wells of ultralow attachment 24-well plates: uncoated MCs (referred to as bare MCs), MCs coated with $(PLO/HA)_8$ (referred to as MC-LbL), and MCs coated with $(PLO/HA)_8$ grafted using 0.1 mM RGD peptide (referred to as MC-RGD 0.1) or 1 mM RGD peptide (referred to as MC-RGD 1). Then, 300 μL of supplemented medium was added to each well and the plates were placed in the incubator for 30 min for conditioning. During this time, hASCs cultured in cell culture flasks were detached from the flask using Accutase and counted using a Burker cell counting chamber. The supernatant was removed from each well, and 300 μL of cell suspension was added, resulting in a final concentration of 3500 cells/well. Well plates were placed in the incubator and manually agitated for 2 min every 28 min for 4 h. Then, each well was rinsed two times with 500 μL of PBS to remove nonadhered cells. The supplemented medium (300 μL) was added to each well, and the plates were incubated for 5 days. The medium was replaced by 500 μL of fresh supplemented medium on day 2. Moreover, on days 0, 2, and 5 of the experiment, metabolic assays were performed in triplicate by incubating the samples for 3 h in 250 μL of reactive medium containing PrestoBlue Cell Viability Reagent (10%). One hundred microliters of supernatant was transferred to a flat-bottom black well plate, and the fluorescence intensity was measured using a TECAN Infinite M1000 microplate reader (560 nm/590 nm excitation/emission). Finally, MCs were retrieved, rinsed twice with 500 μL of PBS, and then stained for cell characterization. For any experiment, the number of independent repetitions of the experiment and the number of replicates used for each repetition are referred to as N and n, respectively.

4.14. Cell Culture in Dynamic Conditions. Cell culture in dynamic conditions was performed using a 125 mL spinner flask equipped with a magnetic ball impellor. To prevent cell and microcarrier adhesion on the inner surface of the spinner flask, it was siliconized with Sigmacote agent (Sigma-Aldrich). After treatment, the spinner flask was thoroughly washed with Milli-Q water to remove the nongrafted product. The surface-modified spinner flask was autoclaved prior to use. Experiments have been performed in triplicate.

MC-RGD 1 prepared from a 50:50 PLLA40/PEG ratio and sieved to obtain a size ranging from 100 to 150 μm was selected for dynamic culture assays. Indeed, such MCs allowed getting stable dispersions in the spinner flask. Sixty milligrams of freshly sterilized MC-RGD 1 was conditioned in 30 mL of fresh medium in a spinner flask for 30 min. Then, the medium was removed and fresh culture medium was added to obtain a final MC concentration of 1 mg mL^{-1}. Cells were seeded at a density of 8365 cells mg^{-1} of MC or 3.5 cells per MC[1]. To ensure cell adhesion, spinner flask agitation was kept intermittent overnight, with a 2 min agitation at 45 rpm, followed by 28 min rest. The following day, the medium with unattached cells was removed and the fresh medium was added. The agitation was then continued at 45 rpm throughout the culture period. The medium was completely replaced every 3 days.

During the cultures in the spinner flask, a tiny fraction of MCs was collected at designated times points for analysis. To maintain consistency, the flask content was mixed by gentle manual agitation and a representative sample was collected from the center of the culture content. One milliliter of the medium containing about 1 mg of MCs was transferred to individual wells of an ultralow adhesion well plate. After MC settling, the supernatant was removed and MCs were rinsed with PBS for further analyses.

The metabolic activity of the cells grown on MCs was also quantified during the culture by the PrestoBlue Cell Viability assay, as described above. For any experiment, the number of independent repetitions of the experiment and the number of replicates used for each repetition are referred to as N and n, respectively.

4.15. Bead-to-Bead Cell Transfer Assays. When the first batch of cells cultured on MC-RGD 1 in the spinner flask was close to 50% confluency (at day 4), fresh MCs were added in the spinner flask at a 50% concentration of the initial MC concentration to perform bead-to-bead transfer. The LbL coating of these fresh MCs was labeled with PAH-rhodamine (deposited as the first layer during the LbL deposition process) to discriminate them from MCs initially present in the flask. Just after the addition of fresh MCs, an intermittent agitation was applied (2 min agitation at 45 rpm, followed by 28 min rest) for 12 h to encourage the transfer of cells from the initial MCs to the new MCs. The agitation was then changed to the continuous mode at 45 rpm for the remaining duration of the culture.

4.16. Cell Viability. Live/dead staining was performed by incubating the sample in a combined solution of calcein-AM (2 μL mL^{-1} in PBS) and ethidium bromide (1 μL mL^{-1} in PBS) for 30 min at room temperature. Stained cells were then imaged by epifluorescence microscopy.

4.17. Nucleus and Cytoskeleton Staining. Cells grown on MCs were fixed in glutaraldehyde aqueous solution (1%) overnight, then permeabilized in 0.1% Triton X-100, and blocked by incubation in PBS containing 5% BSA for 45 min. Staining of actin filaments by Alexa fluor 488 Phalloidine (10 μL mL^{-1} in PBS supplemented with 1% BSA) was performed for 30 min. Then, the samples were rinsed with PBS supplemented with 1% BSA two times for 5 min followed by nucleus staining using DAPI (0.1 μL mL^{-1} in PBS supplemented with 1% BSA) for 10 min. Samples were rinsed again with PBS two times for 5 min before being imaged by CLSM.

4.18. Cell Morphology. Cell grown on MC samples were fixed in 1% (w/w) glutaraldehyde aqueous solution and then serially dehydrated in 20, 40, 60, 80, and 100% (v/v) ethanol/water solutions (5 min each) followed by 10 min immersion in hexamethyldisilazane (HMDS) and overnight drying in a fumehood. The dried samples were sputter-coated with a 10 nm thick layer of gold and imaged by SEM.

■ ASSOCIATED CONTENT

Supporting Information

The Supporting Information is available free of charge at https://pubs.acs.org/doi/10.1021/acsami.0c16875.

SEM images and average sizes of PLLA40 MCs prepared from a 50:50 PLLA40/PEG ratio at different crystallization temperatures; growth curve of (PLO/HA) films on flat surfaces and microscopy images of MCs coated with $(PLO/HA)_8$ labeled with rhodamine; characterization of initial adhesion and viability of h-ASCs on MC-RGD-1 with three different cores; live/dead images of hASCs grown on bare MC, MC-LbL, and MC-RGD-1 in dynamic conditions, on days 1 and 3; characterization of cell viability and proliferation on Cytodex 3 in dynamic conditions; magnetic moment of magnetic

https://dx.doi.org/10.1021/acsami.0c16875
ACS Appl. Mater. Interfaces XXXX, XXX, XXX−XXX

MCs and images showing MC attraction using a magnet (PDF)

AUTHOR INFORMATION

Corresponding Authors

Anne des Rieux − *Institute of Condensed Matter and Nanosciences, Bio and Soft Matter, Universite' catholique de Louvain, 1348 Louvain-la-Neuve, Belgium; Louvain Drug Research Institute, Advanced Drug Delivery and Biomaterials, Universite catholique de Louvain, 1200 Brussels, Belgium*; Email: anne.desrieux@uclouvain.be

Karine Glinel − *Institute of Condensed Matter and Nanosciences, Bio and Soft Matter, Universite' catholique de Louvain, 1348 Louvain-la-Neuve, Belgium*; orcid.org/0000-0002-2000-0169; Email: karine.glinel@uclouvain.be

Authors

Eleana Somville − *Institute of Condensed Matter and Nanosciences, Bio and Soft Matter, Universite' catholique de Louvain, 1348 Louvain-la-Neuve, Belgium*

Anitha Ajith Kumar − *Institute of Condensed Matter and Nanosciences, Bio and Soft Matter, Universite' catholique de Louvain, 1348 Louvain-la-Neuve, Belgium*

Jérôme Guicheux − *Inserm, UMR 1229, RMeS, Regenerative Medicine and Skeleton, Universite de Nantes, ONIRIS, 44042 Nantes, France*

Boris Halgand − *Inserm, UMR 1229, RMeS, Regenerative Medicine and Skeleton, Universite de Nantes, ONIRIS, 44042 Nantes, France; Centre Hospitalier Universitaire de Nantes, 44093 Nantes, France*

Sophie Demoustier-Champagne − *Institute of Condensed Matter and Nanosciences, Bio and Soft Matter, Universite' catholique de Louvain, 1348 Louvain-la-Neuve, Belgium*; orcid.org/0000-0003-3045-6060

Alain M. Jonas − *Institute of Condensed Matter and Nanosciences, Bio and Soft Matter, Universite' catholique de Louvain, 1348 Louvain-la-Neuve, Belgium*; orcid.org/0000-0002-4083-0688

Complete contact information is available at: https://pubs.acs.org/10.1021/acsami.0c16875

Author Contributions

E.S. and A.A.K. contributed equally to this work. The manuscript was written through the contribution of all authors. All authors have given approval to the final version of the manuscript. K.G., A.d.R., A.M.J., and S.D.-C. designed and supervised the study. E.S. and A.A.K. carried out the experiments. J.G. and B.H. contributed to cell culture experiments.

Funding

This research was financially supported by the European Regional Development Fund (ERDF) and Wallonia in the framework of the operational program "Wallonia-2020.EU".

Notes

The authors declare no competing financial interest.

ACKNOWLEDGMENTS

The authors thank A. Mwema and V. Gratpain for help with cell culture, D. Magnin and W. Xu for their help with SEM and CLSM images, respectively, Tristan da Câmara Santa Clara Gomes for the measurement of magnetic properties of the MCs, and M. Kuterbekov for the fruitful discussions. K.G. and A.d.R. are Senior Research Associates of F.R.S.-FNRS.

ABBREVIATIONS

hASCs, human adipose-derived stromal cells
hMSCs, human mesenchymal stromal cells
MC, microcarrier
PLLA, poly(L-lactide)
PEG, poly(ethylene glycol)
LbL, layer-by-layer
HA, hyaluronic acid
PLO, poly(L-ornithine)
SEM, scanning electron microscopy
Sulfo-NHS, *N*-hydroxysulfosuccinimide
EDC, *N*-(3-dimethylaminopropyl)-*N*′-ethylcarbodiimide hydrochloride
CLSM, confocal laser scanning microscopy
MNPs, magnetic nanoparticles

ADDITIONAL NOTE

[1]One milligram of MC prepared from a 50:50 PLLA/PEG ratio at 103 °C contains approximately 2390 ± 157 individual microcarriers according to microscopy analysis. Therefore, an initial seeding density of 8365 cells mg^{-1} of MC means roughly 3.5 cells per microcarrier.

REFERENCES

(1) Heathman, T. R. J.; Nienow, W.; Mccall, M. J.; Coopman, K.; Kara, B.; Hewitt, C. J. The Translation of Cell-Based Therapies: Clinical Landscape and Manufacturing Challenges. *Regener. Med.* **2015**, *10*, 49−64.

(2) dos Santos, F.; Andrade, P. Z.; Abecasis, M. M.; Gimble, J. M.; Chase, L. G.; Campbell, A. M.; Boucher, S.; Vemuri, M. C.; da Silva, C. L.; Cabral, J. M. S. Toward a Clinical-Grade Expansion of Mesenchymal Stem Cells from Human Sources: A Microcarrier-Based Culture System under Xeno-Free Conditions. *Tissue Eng., Part C* **2011**, *17*, 1201−1210.

(3) Kabat, M.; Bobkov, I.; Kumar, S.; Grumet, M. Trends in Mesenchymal Stem Cell Clinical Trials 2004-2018: Is Efficacy Optimal in a Narrow Dose Range? *Stem Cells Transl. Med.* **2020**, *9*, 17−27.

(4) Heathman, T. R. J.; Rafiq, Q. A.; Coopman, K.; Nienow, A. W.; Hewitt, C. J. The Scale-up of Human Mesenchymal Stem Cell Expansion and Recovery. *Bioprocessing for Cell Based Therapies*; Wiley-Blackwell, 2016; pp 91−125.

(5) Merten, O.-W. Advances in Cell Culture: Anchorage Dependence. *Philos. Trans. R. Soc., B* **2015**, *370*, No. 20140040.

(6) Schnitzler, A. C.; Verma, A.; Kehoe, D. E.; Jing, D.; Murrell, J. R.; Der, K. A.; Aysola, M.; Rapiejko, P. J.; Punreddy, S.; Rook, M. S. Bioprocessing of Human Mesenchymal Stem/Stromal Cells for Therapeutic Use: Current Technologies and Challenges. *Biochem. Eng. J.* **2016**, *108*, 3−13.

(7) Spier, M. R.; Porto, L.; Vandenberghe, D. S.; Bianchi, A.; Medeiros, P.; Soccol, C. R. In Application of Different Types of Bioreactors in Bioprocesses. *Bioreactors: Design, Properties and Applications*; Antolli, P. G.; Liu, Z., Eds.; Nova Science Publishers, Inc., 2011; pp 55−90.

(8) Van Wezel, A. L. Growth of Cell-Strains and Primary Cells on Micro-Carriers in Homogeneous Culture. *Nature* **1967**, *216*, 64−65.

(9) Markicheva, E.; Grandfils, C. Microcarriers for Animal Cell Culture. *Biomaterials for Cell Immobilization* **2004**, 734−763.

(10) Rafiq, Q. A.; Coopman, K.; Nienow, A. W.; Hewitt, C. J. Systematic Microcarrier Screening and Agitated Culture Conditions Improve Human Mesenchymal Stem Cell Yield in Bioreactors. *Biotechnol. J.* **2016**, *11*, 473−486.

https://dx.doi.org/10.1021/acsami.0c16875
ACS Appl. Mater. Interfaces XXXX, XXX, XXX−XXX

(11) Jossen, V.; van den Bos, C.; Eibl, R.; Eibl, D. Manufacturing Human Mesenchymal Stem Cells at Clinical Scale: Process and Regulatory Challenges. *Appl. Microbiol. Biotechnol.* **2018**, *102*, 3981−3994.
(12) Tavassoli, H.; Alhosseini, S. N.; Tay, A.; Chan, P. P. Y.; Oh, S. K. W.; Warkiani, M. E. Large-Scale Production of Stem Cells Utilizing Microcarriers: A Biomaterials Engineering Perspective from Academic Research to Commercialized Products. *Biomaterials* **2018**, *181*, 333−346.
(13) Kim, T. K.; Yoon, J. J.; Lee, D. S.; Park, T. G. Gas Foamed Open Porous Biodegradable Polymeric Microspheres. *Biomaterials* **2006**, *27*, 152−159.
(14) Zhou, A.; Ye, Z.; Zhou, Y.; Tan, W. S. Bioactive Poly(ε-Caprolactone) Microspheres with Tunable Open Pores as Microcarriers for Tissue Regeneration. *J. Biomater. Appl.* **2019**, *33*, 1242−1251.
(15) Kankala, R. K.; Zhao, J.; Liu, C. G.; Song, X. J.; Yang, D. Y.; Zhu, K.; Wang, S. B.; Zhang, Y. S.; Chen, A. Z. Highly Porous Microcarriers for Minimally Invasive In Situ Skeletal Muscle Cell Delivery. *Small* **2019**, *15*, No. 1901397.
(16) Nykamp, G.; Carstensen, U.; Muller, B. W. Jet Milling—a New Technique for Microparticle Preparation. *Int. J. Pharm.* **2002**, *242*, 79−86.
(17) Levato, R.; Mateos-timoneda, M. A.; Planell, J. A. Preparation of Biodegradable Polylactide Microparticles via a Biocompatible Procedure. *Macromol. Biosci.* **2012**, *12*, 557−566.
(18) Kuterbekov, M.; Machillot, P.; Lhuissier, P.; Picart, C.; Jonas, A. M.; Glinel, K. Solvent-Free Preparation of Porous Poly(L-Lactide) Microcarriers for Cell Culture. *Acta Biomater.* **2018**, *75*, 300−311.
(19) de Soure, A. M.; Fernandes-platzgummer, A.; Silva, C. L.; Cabral, J. M. S. Scalable Microcarrier-Based Manufacturing of Mesenchymal Stem/Stromal Cells. *J. Biotechnol.* **2016**, *236*, 88−109.
(20) Berry, J. D.; Liovic, P.; Šutalo, I. D.; Stewart, R. L.; Glattauer, V.; Meagher, L. Characterisation of Stresses on Microcarriers in a Stirred Bioreactor. *Appl. Math. Model.* **2016**, *40*, 6787−6804.
(21) Amersham Biosciences. *Microcarrier Cell Culture: Principles and Methods*, 2005.
(22) Younes, H.; Cohn, D. Phase Separation in Poly(Ethylene Glycol)/Poly(Lactic Acid) Blends. *Eur. Polym. J.* **1988**, *24*, 765−773.
(23) Sungsanit, K.; Kao, N.; Bhattacharya, S. N. Properties of Linear Poly(Lactic Acid)/Polyethylene Glycol Blends. *Polym. Eng. Sci.* **2012**, *52*, 108−116.
(24) Li, F. J.; Zhang, S. D.; Liang, J. Z.; Wang, J. Z. Effect of Polyethylene Glycol on the Crystallization and Impact Properties of Polylactide-Based Blends. *Polym. Adv. Technol.* **2015**, *26*, 465−475.
(25) Li, F. J.; Tan, L. C.; Zhang, S. D.; Zhu, B. Compatibility, Steady and Dynamic Rheological Behaviors of Polylactide/Poly(Ethylene Glycol) Blends. *J. Appl. Polym. Sci.* **2016**, *133*, No. 42919.
(26) Keith, H. D.; Padden, F. J. A Phenomenological Theory of Spherulitic Crystallization. *J. Appl. Phys.* **1963**, *34*, 2409−2421.
(27) Farah, S.; Anderson, D. G.; Langer, R. Physical and Mechanical Properties of PLA, and Their Functions in Widespread Applications — A Comprehensive Review. *Adv. Drug Delivery Rev.* **2016**, *107*, 367−392.
(28) Tam, S. K.; Bilodeau, S.; Dusseault, J.; Langlois, G.; Hallé, J.; Yahia, L. H. Biocompatibility and Physicochemical Characteristics of Alginate − Polycation Microcapsules. *Acta Biomater.* **2011**, *7*, 1683−1692.
(29) Darrabie, M. D.; Kendall, W. F.; Opara, E. C. Characteristics of Poly-L-Ornithine-Coated Alginate Microcapsules. *Biomaterials* **2005**, *26*, 6846−6852.
(30) Tian, L.; Prabhakaran, M. P.; Hu, J.; Chen, M.; Besenbacher, F.; Ramakrishna, S. Synergistic Effect of Topography, Surface Chemistry and Conductivity of the Electrospun Nanofibrous Scaffold on Cellular Response of PC12 Cells. *Colloids Surf., B* **2016**, *145*, 420−429.
(31) Jung, S.; Panchalingam, K. M.; Wuerth, R. D.; Rosenberg, L.; Behie, L. A. Large-Scale Production of Human Mesenchymal Stem Cells for Clinical Applications. *Biotechnol. Appl. Biochem.* **2012**, *59*, 106−120.
(32) Kuterbekov, M. Surface Biofunctionalization of 3D Porous Scaffolds for Bone Tissue Engineering. Ph.D. Thesis, Université catholique de Louvain, May 2019.
(33) Richert, L.; Boulmedais, F.; Lavalle, P.; Mutterer, J.; Ferreux, E.; Decher, G.; Schaaf, P.; Voegel, J. C.; Picart, C. Improvement of Stability and Cell Adhesion Properties of Polyelectrolyte Multilayer Films by Chemical Cross-Linking. *Biomacromolecules* **2004**, *5*, 284−294.
(34) Vázquez, C. P.; Boudou, T.; Dulong, V.; Nicolas, C.; Picart, C.; Glinel, K. Variation of Polyelectrolyte Film Stiffness by Photo-Cross-Linking: A New Way to Control Cell Adhesion. *Langmuir* **2009**, *25*, 3556−3563.
(35) Schneider, A.; Francius, G.; Obeid, R.; Schwinté, P.; Hemmerlé, J.; Frisch, B.; Schaaf, P.; Voegel, J. C.; Senger, B.; Picart, C. Polyelectrolyte Multilayers with a Tunable Young's Modulus: Influence of Film Stiffness on Cell Adhesion. *Langmuir* **2006**, *22*, 1193−1200.
(36) Picart, C.; Lavalle, P.; Hubert, P.; Cuisinier, F. J. G.; Decher, G.; Schaaf, P.; Voegel, J. C. Buildup Mechanism for Poly(L-Lysine)/Hyaluronic Acid Films onto a Solid Surface. *Langmuir* **2001**, *17*, 7414−7424.
(37) Hersel, U.; Dahmen, C.; Kessler, H. RGD Modified Polymers: Biomaterials for Stimulated Cell Adhesion and Beyond. *Biomaterials* **2003**, *24*, 4385−4415.
(38) Bacakova, L.; Filova, E.; Rypacek, F.; Svorcik, V.; Stary, V. Cell Adhesion on Artificial Materials for Tissue Engineering. *Physiol. Res.* **2004**, *53*, 35−45.
(39) Bajek, A.; Gurtowska, N.; Olkowska, J.; Kazmierski, L.; Maj, M.; Drewa, T. Adipose-Derived Stem Cells as a Tool in Cell-Based Therapies. *Arch. Immunol. Ther. Exp.* **2016**, *64*, 443−454.
(40) Nagata, T.; Mitsumori, T.; Iwaguro, H. Adipose Tissue-Derived Stem and Regenerative Cells for Tissue Regeneration. *J. Oral Biosci.* **2013**, *55*, 127−131.
(41) Jossen, V.; Schirmer, C.; Mostafa Sindi, D.; Eibl, R.; Kraume, M.; Pörtner, R.; Eibl, D. Theoretical and Practical Issues That Are Relevant When Scaling up HMSC Microcarrier Production Processes. *Stem Cells Int.* **2016**, *2016*, No. 4760414.
(42) Ferrari, C.; Balandras, F.; Guedon, E.; Olmos, E.; Chevalot, I.; Marc, A. Limiting Cell Aggregation during Mesenchymal Stem Cell Expansion on Microcarriers. *Biotechnol. Prog.* **2012**, *28*, 780−787.
(43) Lembong, J.; Kirian, R.; Takacs, J.; Olsen, T.; Lock, L. T.; Rowley, J.; Ahsan, T. Bioreactor Parameters for Microcarrier-Based Human MSC Expansion under Xeno-Free Conditions in a Vertical-Wheel System. *Bioengineering* **2020**, *7*, No. 73.
(44) Eibes, G.; dos Santos, F.; Andrade, P. Z.; Boura, J. S.; Abecasis, M. M. A.; da Silva, C. L.; Cabral, J. M. S. Maximizing the Ex Vivo Expansion of Human Mesenchymal Stem Cells Using a Microcarrier-Based Stirred Culture System. *J. Biotechnol.* **2010**, *146*, 194−197.
(45) Schop, D.; van Dijkhuizen-Radersma, R.; Borgart, E.; Janssen, F. W.; Rozemuller, H.; Prins, H.-J.; De Bruijn, J. D. Expansion of Human Mesenchymal Stromal Cells on Microcarriers: Growth and Metabolism. *J. Tissue Eng. Regener. Med.* **2010**, *4*, 131−140.
(46) Goh, T. K.-P.; Zhang, Z.-Y.; Chen, A. K.-L.; Reuveny, S.; Choolani, M.; Chan, J. K. Y.; Oh, S. K.-W. Microcarrier Culture for Efficient Expansion and Osteogenic Differentiation of Human Fetal Mesenchymal Stem Cells. *BioRes. Open Access* **2013**, *2*, 84−97.
(47) Jorgenson, K. D.; Hart, D. A.; Krawetz, R.; Sen, A. Production of Adult Human Synovial Fluid-Derived Mesenchymal Stem Cells in Stirred-Suspension Culture. *Stem Cells Int.* **2018**, *2018*, No. 8431053.
(48) Wang, Y.; Ouyang, F. Bead-to-Bead Transfer of Vero Cells in Microcarrier Culture. *Bioprocess Eng.* **1999**, *21*, 211−213.
(49) Verbruggen, S.; Luining, D.; van Essen, A.; Post, M. J. Bovine Myoblast Cell Production in a Microcarriers-Based System. *Cytotechnology* **2018**, *70*, 503−512.
(50) Luo, F.; Sun, H.; Geng, T.; Qi, N. Application of Taguchi's Method in the Optimization of Bridging Efficiency between

https://dx.doi.org/10.1021/acsami.0c16875
ACS Appl. Mater. Interfaces XXXX, XXX, XXX−XXX

Confluent and Fresh Microcarriers in Bead-to-Bead Transfer of Vero Cells. *Biotechnol. Lett.* **2008**, *30*, 645−649.
(51) Abeille, F.; Mittler, F.; Obeid, P.; Huet, M.; Kermarrec, F.; Dolega, M. E.; Navarro, F.; Pouteau, P.; Icard, B.; Gidrol, X.; Agache, V.; Picollet-D'hahan, N. Continuous Microcarrier-Based Cell Culture in a Benchtop Microfluidic Bioreactor. *Lab Chip* **2014**, *14*, 3510−3518.
(52) Yu, J.; Shi, J.; Zhang, Y.; Zhang, Y.; Huang, Y.; Chen, Z.; Yang, J. The Replicative Senescent Mesenchymal Stem/Stromal Cells Defect in DNA Damage Response and Anti-Oxidative Capacity. *Int. J. Med. Sci.* **2018**, *15*, 771−781.
(53) Chen, A. K.-L.; Reuveny, S.; Oh, S. K. W. Application of Human Mesenchymal and Pluripotent Stem Cell Microcarrier Cultures in Cellular Therapy: Achievements and Future Direction. *Biotechnol. Adv.* **2013**, *31*, 1032−1046.
(54) Decher, G.; Eckle, M.; Schmitt, J.; Struth, B. Layer-by-Layer Assembled Multicomposite Films. *Curr. Opin. Colloid Interface Sci.* **1998**, *3*, 32−39.

https://dx.doi.org/10.1021/acsami.0c16875
ACS Appl. Mater. Interfaces XXXX, XXX, XXX−XXX